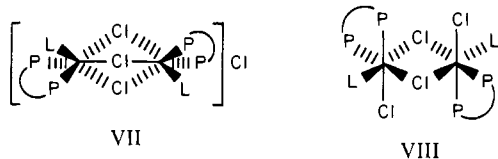


Table II. ^{31}P NMR Parameters

	chem shift ^a	coord chem shift ^b
<i>trans</i> -RuCl ₂ (dppm) ₂	-7.7	15.9
<i>trans</i> -RuCl ₂ (dppc) ₂	44.3	56.8
<i>trans</i> -RuCl ₂ (dppp) ₂	-5.0	12.3
<i>cis</i> -RuCl ₂ (dppp) ₂	42.0, -2.7 (<i>J</i> = 31.5 Hz)	59.3, 14.6

^a In CH₂Cl₂ at 303 K. ^b $\delta[\text{RuCl}_2(\text{chelate})_2] - \delta(\text{chelate})$.

all *J* values indicate *cis* stereochemistry. Two structures consistent with these facts are shown as VII and VIII.



Reaction of RuCl₂L₃ with Ph₂PCH₂PPh₂ (dppm). Reaction of equimolar amounts of RuCl₂L₃ and dppm produces *trans*-RuCl₂(dppm)₂ as the major product. Again, free PPh₃ and unreacted RuCl₂L₃ are evident, but free and monodentate dppm are absent. No ABX pattern is observed (i.e., RuCl₂(PPh₃)(dppm) is not produced), nor are there any other singlet resonances. A 6% yield of an AB pattern consistent with VI is also observed.

Conclusion

The $^{31}\text{P}\{^1\text{H}\}$ NMR spectra of these RuCl₂(Ph₂P(CH₂)_{*n*}PPh₂)₂ complexes (Table II) warrant no further dis-

cussion other than their adherence to the ΔR rule,¹² which notes that phosphorus ligands involved in chelate rings reveal coordination chemical shifts (Δ) outside the range normally predicted by the $\alpha = A\delta F + B$ relationship.¹³ In qualitative terms, one observes that, compared to a nonchelated, *cis*-disubstituted analogue, four-membered rings are shielded more than six-membered rings and five-membered rings are deshielded. This trend is also evident in comparing VI (dppe) with II (dppb). The large downfield shift for phosphorus *trans* to chlorine in *cis*-RuCl₂(dppp)₂ is noteworthy. The same effect is evident in isoelectronic *cis*-IrCl₂(dppe)₂.¹⁴

Neither dppe or dppm forms coordinatively unsaturated RuCl₂(PPh₃)(chelate). This is presumably a function of chelate bite angle. As this angle becomes smaller, the coordination sphere about ruthenium becomes less sterically congested and RuCl₂(PPh₃)(chelate), once formed, is accessible to further reaction to form coordinatively saturated monomeric or dimeric products.

Acknowledgment. We gratefully acknowledge support of this work by the Research Corp. and the National Science Foundation (Grant GP-38641X).

Registry No. I, 88496-72-4; II, 88496-73-5; [RuCl₂(dppb)_{1.5}]₂, 55669-36-8; *trans*-RuCl₂(dppp)₂, 55669-28-8; *trans*-RuCl₂(dppe)₂, 19349-72-5; *trans*-RuCl₂(dppm)₂, 38800-82-7; RuCl₂(PPh₃)₃, 15529-49-4.

(12) Garrou, P. E. *Chem. Rev.* **1981**, *81*, 229.

(13) Mann, B. E.; Masters, C.; Shaw, B. L. *J. Chem. Soc. A* **1971**, 1104.

(14) Miller, J. S.; Caulton, K. G. *J. Am. Chem. Soc.* **1975**, *97*, 1067.

Contribution from the Chemistry Department,
Faculty of Science, Australian National University, Canberra 2600, Australia

Oxo-Bridged Mixed-Oxidation-State Complexes of Molybdenum: Preparation, Properties, and X-ray Structure of [Mo₂O(S₂CNET₂)₆]BF₄ and Related Compounds

JOHN A. BROOMHEAD,* META STERNS, and CHARLES G. YOUNG¹

Received May 17, 1983

The oxo-bridged mixed-oxidation-state compound [Mo₂O(S₂CNET₂)₆]BF₄ has been prepared by the reaction of [MoO(S₂CNET₂)₃]BF₄ and triphenylphosphine and fully characterized by single-crystal X-ray diffraction. The compound crystallizes in the monoclinic space group *C2/c* with *a* = 13.24 (1) Å, *b* = 30.86 (4) Å, *c* = 12.42 (1) Å, β = 97.89 (4)°, and *Z* = 4. The structure was refined by full-matrix least-squares methods to final residual values of *R* = 0.035 and *R*_w = 0.041 on the basis of 3131 independent reflections. The cation contains two pentagonal-bipyramidal (asymmetric) units linked by an almost linear (Mo-O-Mo = 175.6 (2)°) bridging oxo ligand having Mo-O bond lengths of 1.848 (2) Å. It is the first dithiocarbamate complex of molybdenum to exhibit oxo bridging in the absence of terminal oxo ligands and is the first dinuclear seven-coordinate molybdenum complex in which an axial oxygen atom functions as the bridging group. The compound is paramagnetic ($\mu_{\text{eff}} = 2.17 \mu_{\text{B}}$), is a 1:1 electrolyte in methanol, and shows an intervalence-transfer band at 1310 nm ($\epsilon \approx 1100 \text{ L cm}^{-1} \text{ mol}^{-1}$). The detailed crystal and molecular structure, electrochemistry, and spectral characteristics of the compound are presented and discussed as is the nature of the mixed oxidation state. The preparation and properties of the analogous dimethyldithiocarbamate complex and of the PF₆⁻, ClO₄⁻, and Cl⁻ salts of both complexes are also described.

Introduction

Dinuclear molybdenum centers have been postulated for xanthine oxidase, sulfite oxidase, and nitrate reductase, and their participation in the catalytic cycles of these enzymes has been suggested.² For a dinuclear active-site model, the mononuclear Mo(V) characteristics of the enzyme ESR signals^{3,4}

may be understood in terms of mixed-oxidation-state centers [Mo(IV, V) or Mo(V, VI)] in which the unpaired electron is localized on only one molybdenum atom. In terms of enzyme model studies, however, there is a notable lack of simple complexes that adequately model these mixed-oxidation-state centers. At present, the majority of mixed-oxidation-state

(1) Abstracted from: Young, C. G. Ph.D. Dissertation, Australian National University, May 1982. Present address: Chemistry Department, University of British Columbia, Vancouver, Canada.
(2) Wentworth, R. A. D. *Coord. Chem. Rev.* **1976**, *18*, 1.

(3) Bray, R. C. In "The Enzymes"; Boyer, P. D., Ed.; Academic Press: New York, 1975; Vol. 12, p 299.

(4) Bray, R. C. In "Biological Magnetic Resonance"; Berliner, L. J., Reuben, J., Eds.; Plenum Press: New York, 1980; Vol. 2, p 45.

complexes of molybdenum are of the oxyanion type, represented by the Mo(IV, VI) compound $K_6[Mo_3O_6(CN)_6] \cdot 2H_2O^5$ and the Mo(V, VI) tetramer $Mo_4O_6Cl_4(O-n-Pr)_6$.⁶ Also, Cotton et al.⁷ have studied the Mo(II, III) compound $K_3[Mo_2(SO_4)_4] \cdot 3.5H_2O$ and concluded that the unpaired electron is evenly distributed over two magnetically equivalent molybdenum atoms. More recently, the complexes $[Mo(\eta-C_5H_4R)_2(\mu-X)_2MoX_2]_2$ ($R = H, Me, n-Bu$; $X = O, S$) have been reported.⁸

In contrast, mixed-oxidation-state molybdenum complexes containing the biologically significant sulfur donor ligands are rare. Transient Mo(IV, V) complexes have been proposed to exist in solution upon the electrochemical⁹ and chemical¹⁰ reduction of dinuclear Mo(V) complexes, but their instability has prevented isolation and further characterization. Recently the Mo(IV, V) complex $[Mo_2O_3(S_2CNET_2)_4]^-$ was stabilized in a mixed crystal of composition $(H_2O)_2[Mo_2O_3(S_2CNET_2)_4]$.¹¹ In this case, the ESR spectra were consistent with the localization of the unpaired electron on one molybdenum atom only. In a previous communication we reported the first example of an oxo-bridged dinuclear mixed-oxidation-state molybdenum complex in which the coligands are all sulfur donors.¹² We report here the detailed solid-state structure of $[Mo_2O(S_2CNET_2)_6]BF_4$ (**1**) and the physical and spectroscopic characterization of this and related compounds.

Experimental Section

Materials and Methods. The compounds $[MoO(S_2CNR_2)_3]X$ ($R = Me, Et$; $X = BF_4^-, PF_6^-, ClO_4^-$) were prepared by the reaction of *cis*- $MoO_2(S_2CNR_2)_2$ and ca. 65% aqueous HX in acetone solvent.¹³ $MoCl(S_2CNET_2)_3$ was prepared by the method of Bishop et al.¹⁴ The preparation and solution study of the compounds were performed under an atmosphere of dinitrogen with dried and deoxygenated solvents. Microanalyses were performed by the Australian National University Microanalytical Service.

Preparation of Compounds. (μ -Oxo)hexakis(*N,N*-diethyldithiocarbamate)dimolybdenum(IV,V) Tetrafluoroborate, $[Mo_2O(S_2CNET_2)_6]BF_4$ (1**).** A mixture of $[MoO(S_2CNET_2)_3]BF_4$ (0.3 g, 0.47 mmol) and triphenylphosphine (0.123 g, 0.47 mmol) was dissolved in methanol (25 mL), and the resulting solution was stirred for 3 h. After cooling at 2 °C, the mixture was filtered in air and the green-black crystals obtained were washed with methanol/ether (1:10) and dried under vacuum; yield 0.18 g (65%). Anal. Calcd for $C_{30}H_{60}BF_4Mo_2N_6OS_{12}$: C, 30.4; H, 5.1; Mo, 16.2; N, 7.1; P, nil; S, 32.5. Found: C, 30.4; H, 5.1; Mo, 16.0; N, 7.0; P, nil; S, 32.7. Molar conductivity: $\Lambda_M = 82 \Omega^{-1} cm^2 mol^{-1}$. Magnetic moment: solid, $\mu_{eff} = 2.17 \mu_B$ (296.4 K); $CHCl_3/Me_4Si$ solution, $\mu_{eff} = 2.10 \mu_B$ (301.0 K). Infrared spectrum (cm^{-1}): $\nu(CN)$ 1510 s; $\nu(NC_2)$ 1150 m; $\nu(C=S)$ 1000 w; $\nu(CSS)$ 935 w, 910 w, 905 w; $\nu_{as}(MoOMo)$ 665 w, br; $\nu(Mo-S)$ 365 w; BF_4^- 1070 s, 530 w, 520 w. UV-visible spectrum (CH_3OH) (λ_{max} , nm (ϵ , L $cm^{-1} mol^{-1}$)) 677 (2440), 497 (19 200), 440 (14 400), 410 (13 400).

Electrochemistry at a HMDE ($Ag/0.1 M AgNO_3 (CH_3CN)$ reference), $E_0 = -0.77 V$ ($-0.44 V$ vs. SCE): at 100 mV/s scan rate, $E_p = 75 mV$, $i_{ox}/i_{red} = 0.95$; at 50 mV/s scan rate, $E_p = 78 mV$, $i_{ox}/i_{red} = 0.95$; at 20 mV/s scan rate, $E_p = 78 mV$, $i_{ox}/i_{red} = 1.00$. Electrochemistry at a Pt electrode ($Ag/AgCl$ reference), $E_0 = -0.43 V$ ($-0.24 V$ vs. SCE): at 100 mV/s scan rate, $E_p = 70 mV$, $i_{ox}/i_{red} = 0.98$. At Pt, irreversible oxidation waves occur at +0.12, +0.45, and +0.99 V and are accompanied by an irreversible reduction wave at +0.29 V.

(μ -Oxo)hexakis(*N,N*-diethyldithiocarbamate)dimolybdenum(IV,V) Hexafluorophosphate and (μ -Oxo)hexakis(*N,N*-diethyldithiocarbamate)dimolybdenum(IV,V) Perchlorate. These compounds were prepared from corresponding salts of $[MoO(S_2CNET_2)_3]^+$ by methods analogous to that used for **1**. $[Mo_2O(S_2CNET_2)_6]PF_6$ (**2**) was isolated in 67% yield. Anal. Calcd for $C_{30}H_{60}F_6Mo_2N_6OPS_{12}$: C, 29.5; H, 5.0; Mo, 15.7; N, 6.9; P, 2.5; S, 31.5. Found: C, 29.3; H, 5.0; Mo, 15.8; N, 6.8; P, 2.4; S, 31.5. Molar conductivity: $\Lambda_0 = 76 \Omega^{-1} cm^2 mol^{-1}$. Infrared spectrum (cm^{-1}): as for **1** except $\nu_{as}(MoOMo)$ 670 w; $\nu(Mo-S)$ 360; PF_6^- 840 vs, 560 s. $[Mo_2O(S_2CNET_2)_6]ClO_4$ (**3**) was isolated in 50% yield. Anal. Calcd for $C_{30}H_{60}ClMo_2N_6O_5S_{12}$: C, 30.1; H, 5.0; Cl, 3.0; Mo, 16.0; N, 7.0; O, 6.7; S, 32.1. Found: C, 30.1; H, 5.0; Cl, 3.0; Mo, 15.8; N, 7.0; O, 7.0; S, 32.2. Molar conductivity: $\Lambda_M = 81 \Omega^{-1} cm^2 mol^{-1}$. Infrared spectrum (cm^{-1}): as for **1** except for $\nu_{as}(MoOMo)$ 660 w; $\nu(Mo-S)$ 360 w; ClO_4^- 1090 s, 830 w.

(μ -Oxo)hexakis(*N,N*-diethyldithiocarbamate)dimolybdenum(IV,V) Chloride, $[Mo_2O(S_2CNET_2)_6]Cl$ (4**).** A suspension of $MoCl(S_2CNET_2)_3$ (1.37 g, 2.38 mmol) in methanol (50 mL) was stirred in air for 4 h and then filtered to yield a clear orange solution of $[MoO(S_2CNET_2)_3]Cl$.¹⁵ This was deoxygenated and added to triphenylphosphine (0.63 g, 2.40 mmol) under dinitrogen. After the mixture was stirred for 4 h, the volume of the solution was reduced to 15–20 mL. Ether (350 mL) was added and the solution cooled at 2 °C for 2 h to obtain green-black crystals of **4**; yield 0.73 g (52%). Anal. Calcd for $C_{30}H_{60}ClMo_2N_6OS_{12}$: C, 31.8; H, 5.3; Cl, 3.1; Mo, 16.9; N, 7.4; S, 33.9. Found: C, 31.9; H, 5.5; Cl, 2.9; Mo, 16.9; N, 7.4; S, 33.8. Molar conductivity: $\Lambda_M = 76 \Omega^{-1} cm^2 mol^{-1}$. Magnetic moment: solid, $\mu_{eff} = 2.01 \mu_B$ (294.5 K). Infrared spectrum (cm^{-1}): as for **1** except $\nu_{as}(MoOMo)$ 675 w; no anion bands.

The *N,N*-dimethyldithiocarbamate analogues were also prepared by the above methods except using reaction times of 24 h. The compounds are very insoluble and are difficult to obtain analytically pure. Their infrared spectra are characterized by the bands $\nu(CN)$ 1545 s, $\nu(NC_2)$ 1250 m, and $\nu(C=S)$ 1050 cm^{-1} and obscured by BF_4^- and ClO_4^- bands, $\nu(CSS)$ 935 w and 905 cm^{-1} , $\nu_{as}(MoOMo)$ 675 w, br cm^{-1} , br $\nu(Mo-S)$ 365 cm^{-1} , and anion bands.

Physical Measurements. Solution electrical conductivities (methanol, 25 °C) were measured by using a Philips PR9500 bridge and sample concentrations of $10^{-3} M$. Solid-state and solution magnetic susceptibilities were measured by the Gouy¹⁶ ($Hg[Co(NCS)_4]$ calibrant) and Evans NMR¹⁷ methods, respectively. Molar susceptibilities were corrected for diamagnetism with use of the appropriate Pascal constants.¹⁸ Infrared spectra were recorded on a Perkin-Elmer 683 spectrophotometer as CsI disks. For near-infrared spectra, a Cary 14 spectrophotometer and quartz solution cells were employed. The UV-visible spectra were recorded on a Cary 219 spectrophotometer using quartz cells. Electrochemical experiments (at 20 °C) employed $10^{-3} M$ solutions of **1** in 0.1 M Et_4NClO_4/CH_3CN . Cyclic voltammograms at a HMDE (PAR Model 303 SMDE) were recorded on a PAR Model 170 electrochemistry system using a $Ag/0.1 M AgNO_3 (CH_3CN)$ reference electrode (+0.337 V vs. SCE) and a platinum-wire auxiliary electrode. Cyclic voltammograms at a platinum working electrode were recorded on a PAR Model 172/175/179 potentiostat/galvanostat, universal programmer, and digital coulometer. The experiment used an $Ag/AgCl$ reference electrode (+0.19 V vs. SCE) and a platinum-wire auxiliary electrode. Coulometry was performed with an AMEL Model 551 potentiostat, Model 731 digital integrator, and a PAR Model 377 coulometry

- (5) Van de Poel, J.; Neumann, H. M. *Inorg. Chem.* **1968**, *7*, 2086.
- (6) Beaver, J. A.; Drew, M. G. B. *J. Chem. Soc., Dalton Trans.* **1973**, 1376. See: Koch, S. A.; Lincoln, S. *Inorg. Chem.* **1982**, *21*, 2904.
- (7) Cotton, F. A.; Frenz, B. A.; Pederson, E.; Webb, T. R. *Inorg. Chem.* **1975**, *14*, 391.
- (8) Adam, G. J. S.; Green, M. L. H. *J. Organomet. Chem.* **1981**, *208*, 299.
- (9) (a) Howie, J. K.; Sawyer, D. T. *Inorg. Chem.* **1976**, *15*, 1892. (b) Schultz, F. A.; Ott, V. R.; Rolison, D. W.; Bravard, D. C.; McDonald, J. W.; Newton, W. E. *Ibid.* **1978**, *17*, 1758. (c) Bradbury, J. R.; Masters, A. F.; McDonnell, A. C.; Brunett, A. A.; Bond, A. M.; Wedd, A. G. *J. Am. Chem. Soc.* **1981**, *103*, 1959 and references therein.
- (10) Haight, G. P.; Wolterman, G.; Imamura, T.; Hummel, P. In "Proceedings of the Second International Conference on the Chemistry and Uses of Molybdenum"; Mitchel, P. C. H.; Seaman, A., Eds.; Climax Molybdenum Co.: London, **1976**, p 60.
- (11) Garner, C. D.; Howlader, N. C.; Mabbs, F. E.; McPhail, A. T.; Onan, K. D. *J. Chem. Soc., Dalton Trans.* **1979**, 962.
- (12) Broomhead, J. A.; Sterns, M.; Young, C. G. *J. Chem. Soc., Chem. Commun.* **1981**, 1262.
- (13) Young, C. G. Ph.D. Thesis, Australian National University, May 1982. Young, C. G.; Broomhead, J. A.; Boreham, C. J. *J. Chem. Soc., Dalton Trans.* **1983**, 2135.
- (14) Bishop, M. W.; Chatt, J.; Dilworth, J. R. *J. Organomet. Chem.* **1974**, *73*, C59.

- (15) Bishop, M. W.; Chatt, J.; Dilworth, J. R.; Hursthouse, M. B.; Motevalli, M. In ref 10, p 252.
- (16) Figgis, B. N.; Nyholm, R. S. *J. Chem. Soc.* **1958**, 4190.
- (17) Evans, D. F. *J. Chem. Soc.* **1959**, 2003.
- (18) Figgis, B. N.; Lewis, J. In "Techniques of Inorganic Chemistry"; Jonaassen, H. B.; Weissberger, A., Eds.; Wiley-Interscience: New York, **1965**; Vol. 4, p 137.

Table I. Crystallographic Study of $[\text{Mo}_2\text{O}(\text{S}_2\text{CNET}_2)_6]\text{BF}_4$

formula	$\text{C}_{30}\text{H}_{60}\text{BF}_4\text{Mo}_2\text{N}_6\text{OS}_{12}$
fw	1183.30
cryst syst	monoclinic
space group	$C2/c$
unit cell dimens (at $21 \pm 1^\circ\text{C}$)	$a = 13.24 (1) \text{ \AA}$ $b = 30.86 (4) \text{ \AA}$ $c = 12.42 (1) \text{ \AA}$ $\beta = 97.89 (4)^\circ$
V	5027 \AA^3
$D(\text{measd})$	1.563 g cm^{-3} (by flotation in CCl_4 at 37.5°C)
Z	4
$D(\text{calcd})$	1.561 g cm^{-3}
radiation	Mo $K\alpha$, graphite crystal monochromated ($\lambda = 0.7107 \text{ \AA}$)
cryst size	$0.04 \times 0.13 \times 0.50 \text{ mm}$
refln forms recorded	($\pm h, k, l$)
angular range	$4^\circ < 2\theta(\text{Mo } K\alpha) < 50^\circ$
scan type	$\theta-2\theta$
scan width	$(1.6 \pm 0.68 \tan \theta)^\circ$
total no. of obsd reflns	4235
no. of unique reflns with $I > 2\sigma(I)$	3131
method of struct soln	MULTAN direct-methods package
least-squares refinement	block diagonal and full matrix
function minimized	$\sum w F_o - F_c ^2$
final weights for refinement	$w = 1/\sigma_2^2$
R^a	0.035
R_w^b	0.041
quality-of-fit indicator ^c	1.054
largest shift/esd in final cycle	0.1, 0.3 for BF_4^-

^a $R = \sum w||F_o| - |F_c||^2 / \sum |F_o|$. ^b $R_w = [\sum w(|F_o| - |F_c|)^2 / \sum w|F_o|^2]^{1/2}$. ^c Quality-of-fit = $[\sum w(|F_o| - |F_c|)^2 / (N_{\text{observns}} - N_{\text{parameters}})]^{1/2}$.

system. A mercury-pool working electrode, a platinum-gauze auxiliary electrode, and a $\text{Ag}/0.1 \text{ M AgNO}_3$ (CH_3CN) reference electrode was employed.

Crystallographic Study. Relevant information is given in Table I. Air-stable crystals of **1** were obtained by slow evaporation of a methanol solution under anaerobic conditions. The reflection conditions determined from precession photographs were hkl for $h + k = 2n$ and $h0l$ for $l = 2n$, which are common to space groups Cc (C_2 ,⁴ No. 9¹⁹) and $C2/c$ (C_{2h} ,⁶ No. 15¹⁹). The latter space group was chosen since the $|E|$ statistics were indicative of a centrosymmetric space group. The data were collected at 20°C on a Philips PW1100/20 automatic four-circle diffractometer using graphite-monochromated Mo $K\alpha$ radiation. Standard reflections measured at regular intervals during the course of the experiment showed no overall trend with time. The 4235 symmetry-permitted reflections collected were converted to structure amplitudes in the usual way. No absorption or extinction corrections were applied (linear absorption coefficient 10.10 cm^{-1}).

Structure Solution and Refinement. The structure was solved by direct methods using MULTAN-77. Anomalous dispersion corrections were added to the neutral-atom scattering factors of Mo and S atoms. As required by symmetry restrictions, the x , z , β_{12} , and β_{23} parameters of O and B atoms were fixed at $0.0a$, $0.25c$, 0.0 , and 0.0 , respectively.²⁰ Isotropic refinement by full-matrix least squares was followed by anisotropic refinement, which converged with a residual R index of 0.038 . Although in the sterically favored staggered positions, the experimental hydrogen atoms located at this stage yielded somewhat distorted methyl group geometries. Hence, hydrogen atoms were inserted in calculated positions, on the assumptions of fully staggered conformations, C-H bond distances of 0.95 \AA , and hydrogen isotropic thermal parameters 10% greater than those of the carbon atoms to which they are bonded. The hydrogen parameters were included in but not refined by subsequent calculations. Final refinement used the weighting scheme $w = 1/\sigma_2^2$ where σ_2 was calculated from $\sigma_2 = [\sigma_1^2 + 0.25(pF_o)^2]^{1/2}$ by using an experimental uncertainty factor of $P = 0.045$.²¹ The final residual indices were $R = 0.035$ and $R_w =$

Table II. Final Positional Parameters for the Asymmetric Unit of $[\text{Mo}_2\text{O}(\text{S}_2\text{CNET}_2)_6]\text{BF}_4$

atom	x/a	y/b	z/c
Mo	-0.0053 (1)	0.3480 (1)	0.3978 (1)
S(1)	-0.0392 (1)	0.3637 (1)	0.5892 (1)
S(2)	-0.1057 (1)	0.4159 (1)	0.3992 (1)
S(3)	0.1250 (1)	0.4071 (1)	0.4115 (1)
S(4)	0.1700 (1)	0.3191 (1)	0.4541 (1)
S(5)	-0.0232 (1)	0.2672 (1)	0.4143 (1)
S(6)	-0.1887 (1)	0.3240 (1)	0.3609 (1)
O	0.0	0.3457 (1)	0.25
N(1)	-0.1663 (3)	0.4317 (1)	0.5919 (3)
N(2)	0.3186 (3)	0.3788 (1)	0.4527 (3)
N(3)	-0.2144 (3)	0.2377 (1)	0.3615 (3)
C(1)	-0.1105 (3)	0.4071 (1)	0.5367 (3)
C(2)	0.2197 (3)	0.3702 (1)	0.4411 (3)
C(3)	-0.1525 (3)	0.2712 (1)	0.3756 (3)
C(4)	-0.1770 (4)	0.4233 (2)	0.7068 (4)
C(5)	-0.2313 (4)	0.4657 (2)	0.5371 (4)
C(6)	0.3528 (4)	0.4235 (2)	0.4411 (4)
C(7)	0.3968 (3)	0.3451 (2)	0.4778 (4)
C(8)	-0.1765 (4)	0.1931 (2)	0.3698 (4)
C(9)	-0.3247 (3)	0.2434 (2)	0.3315 (4)
C(10)	-0.1454 (6)	0.4596 (2)	0.7804 (5)
C(11)	-0.3334 (4)	0.4494 (2)	0.4857 (5)
C(12)	0.3562 (4)	0.4368 (2)	0.3257 (5)
C(13)	0.4595 (4)	0.3380 (2)	0.3885 (4)
C(14)	-0.1426 (5)	0.1774 (2)	0.2661 (5)
C(15)	-0.3604 (4)	0.2335 (2)	0.2149 (5)
B	0.0	0.0570 (5)	0.25
F(1)	0.0403 (14)	0.0733 (8)	0.1797 (16)
F(2)	-0.0975 (7)	0.0446 (5)	0.2169 (10)
F(1B)	-0.0140 (16)	0.0253 (3)	0.1783 (10)
F(2B)	-0.0052 (16)	0.0875 (4)	0.1761 (12)

Table III. Selected Bond Lengths, Bond Angles, and Interatomic Distances for the Coordination Group of $[\text{Mo}_2\text{O}(\text{S}_2\text{CNET}_2)_6]\text{BF}_4$

Distances, \AA			
Mo-O	1.848 (2)	O...S(6)	3.087 (1)
Mo-S(1)	2.526 (2)	S(1)-S(2)	2.893 (1)
Mo-S(2)	2.484 (3)	S(1)-S(3)	3.565 (2)
Mo-S(3)	2.500 (2)	S(1)-S(4)	3.696 (2)
Mo-S(4)	2.495 (2)	S(1)-S(5)	3.710 (2)
Mo-S(5)	2.516 (2)	S(1)-S(6)	3.451 (2)
Mo-S(6)	2.519 (2)	S(2)-S(3)	3.050 (2)
O...S(1)	4.351 (1)	S(2)-S(6)	3.054 (2)
O...S(2)	3.287 (3)	S(3)-S(4)	2.815 (2)
O...S(3)	3.073 (2)	S(4)-S(5)	3.022 (2)
O...S(4)	3.256 (1)	S(5)-S(6)	2.815 (2)
O...S(5)	3.210 (3)		
Angles, deg			
O-Mo-S(1)	167.96 (8)	S(1)-Mo-S(5)	94.74 (4)
O-Mo-S(2)	97.62 (9)	S(1)-Mo-S(6)	86.32 (4)
O-Mo-S(3)	88.60 (8)	S(2)-Mo-S(3)	75.45 (4)
O-Mo-S(4)	95.97 (5)	S(3)-Mo-S(4)	68.59 (4)
O-Mo-S(5)	93.44 (9)	S(4)-Mo-S(5)	73.60 (4)
O-Mo-S(6)	88.57 (4)	S(5)-Mo-S(6)	67.97 (4)
S(1)-Mo-S(2)	70.53 (4)	S(2)-Mo-S(6)	75.24 (8)
S(1)-Mo-S(3)	90.36 (4)	Mo-O-Mo	175.6 (2)
S(1)-Mo-S(4)	94.81 (4)		

0.041. The largest peak in the final difference Fourier synthesis was 0.4 e \AA^{-3} .

All calculations were performed on a UNIVAC 1100/42 computer using the ANUCRYS crystallographic program library.²² The atomic scattering factors used were taken from Doyle and Turner²³ and Stewart et al.²⁴ (for hydrogen), and the anomalous dispersion factors

(19) "International Tables for X-Ray Crystallography", 3rd ed.; Henry, N. F. M., Lonsdale, K., Eds.; Kynoch Press: Birmingham, England 1969; p 101.

(20) Peterse, W. J. A.; Palm, J. H. *Acta Crystallogr.* **1966**, *20*, 147.

(21) Busing, W. R.; Levy, H. A. *J. Chem. Phys.* **1957**, *26*, 563. Corfield, P. W. R.; Doedens, R. J.; Ibers, J. A. *Inorg. Chem.* **1967**, *6*, 197.

(22) McLaughlin, G. M.; Taylor, D.; Whimp, P. O. "The ANUCRYS Structure Determination Package", Research School of Chemistry, Australian National University, Canberra, ACT 2600, Australia. Mau, A. W.-H.; Whimp, P. O. *J. Am. Chem. Soc.* **1979**, *101*, 2363.

(23) Doyle, P. A.; Turner, P. S. *Acta Crystallogr., Sect. A* **1968**, *A 24*, 390.

(24) Stewart, R. F.; Davidson, E. R.; Simpson, W. T. *J. Chem. Phys.* **1965**, *42*, 3175.

Table IV. Bond Lengths, Bond Angles, and Interatomic Distances for the *N,N*-Diethyldithiocarbamate Ligands

ligand I		ligand II		ligand III		av
Distances, Å						
S(1)··S(2)	2.893 (1)	S(3)··S(4)	2.815 (2)	S(5)··S(6)	2.815 (2)	2.841 ± 0.052
S(1)-C(1)	1.716 (4)	S(3)-C(2)	1.697 (4)	S(5)-C(3)	1.718 (4)	1.716 ± 0.022
S(2)-C(1)	1.738 (4)	S(4)-C(2)	1.724 (5)	S(6)-C(3)	1.703 (5)	
C(1)-N(1)	1.316 (5)	C(2)-N(2)	1.324 (5)	C(3)-N(3)	1.316 (5)	1.319 ± 0.005
N(1)-C(4)	1.476 (5)	N(2)-C(6)	1.465 (6)	N(3)-C(8)	1.465 (6)	1.468 ± 0.008
N(1)-C(5)	1.464 (6)	N(2)-C(7)	1.469 (6)	N(3)-C(9)	1.467 (6)	
C(4)-C(10)	1.471 (8)	C(6)-C(12)	1.498 (7)	C(8)-C(14)	1.502 (8)	1.492 ± 0.021
C(5)-C(11)	1.500 (8)	C(7)-C(13)	1.490 (7)	C(9)-C(15)	1.493 (7)	
Angles, deg						
Mo-S(1)-C(1)	87.2 (1)	Mo-S(3)-C(2)	90.4 (1)	Mo-S(5)-C(3)	90.4 (1)	89.5 ± 2.2
Mo-S(2)-C(1)	88.1 (1)	Mo-S(4)-C(2)	90.0 (1)	Mo-S(6)-C(3)	90.7 (1)	
S(1)-C(1)-S(2)	113.8 (2)	S(3)-C(2)-S(4)	110.7 (2)	S(5)-C(3)-S(6)	110.7 (2)	111.8 ± 2.0
S(1)-C(1)-N(1)	124.8 (3)	S(3)-C(2)-N(2)	125.4 (3)	S(5)-C(3)-N(3)	123.9 (3)	124.1 ± 2.7
S(2)-C(1)-N(1)	121.4 (3)	S(4)-C(2)-N(2)	123.9 (3)	S(6)-C(3)-N(3)	125.3 (3)	
C(1)-N(1)-C(4)	122.5 (4)	C(2)-N(2)-C(6)	119.5 (4)	C(3)-N(3)-C(8)	121.9 (4)	121.4 ± 1.9
C(1)-N(1)-C(5)	120.5 (4)	C(2)-N(2)-C(7)	122.6 (4)	C(3)-N(3)-C(9)	121.2 (4)	
N(1)-C(4)-C(10)	114.2 (5)	N(2)-C(6)-C(12)	113.8 (4)	N(3)-C(8)-C(14)	112.5 (4)	113.4 ± 0.9
N(1)-C(5)-C(11)	113.3 (5)	N(2)-C(7)-C(13)	113.2 (4)	N(3)-C(9)-C(15)	113.2 (4)	

were taken from Cromer and Liberman.²⁵ Final atomic coordinates for the non-hydrogen atoms in the asymmetric unit of **1** are given in Table II. Bond lengths and angles within the coordination group and the dithiocarbamate ligands are given in Tables III and IV, respectively.

Results and Discussion

Properties, Infrared Spectra, and Electrochemistry. The reaction of $[\text{MoO}(\text{S}_2\text{CNR}_2)_3]\text{X}$ compounds and PPh_3 in methanol under anaerobic conditions results in the formation of the new green-black dichroic compounds $[\text{Mo}_2\text{O}(\text{S}_2\text{CNR}_2)_6]\text{X}$ ($\text{R} = \text{Me, Et, X} = \text{BF}_4^-, \text{PF}_6^-, \text{ClO}_4^-$; $\text{R} = \text{Et, X} = \text{Cl}^-$). The compounds, which are air stable in the solid state but rapidly oxidized in solution, are formulated on the basis of analysis and a variety of physical measurements. The molar conductivities of the soluble $\text{R} = \text{Et}$ compounds are typical of 1:1 electrolytes²⁶ and the presence of one unpaired electron per $[\text{Mo}_2\text{O}(\text{S}_2\text{CNEt}_2)_6]^+$ complex (for a $\text{Mo}^{\text{IV}}\text{Mo}^{\text{V}}$ system) is indicated by magnetic susceptibility measurements in both the solid and solution states.

The infrared spectra of the compounds show bands characteristic of bidentate dithiocarbamate ligands and the respective counteranions. A weak band at ca. 675 cm^{-1} is tentatively assigned to the $\nu_{\text{as}}(\text{MoOMo})$ vibration although we have been unable to prepare highly enriched $\mu\text{-}^{18}\text{O}$ complexes in order to confirm this assignment. The only dinuclear $\mu\text{-oxo}$ complexes available for IR comparison contain either $\text{Mo}(\text{V})$ or $\text{Mo}(\text{III})$ as well as terminal oxo ligands. The $\nu_{\text{as}}(\text{MoOMo})$ bands in these complexes occur in the $706\text{--}765\text{-}$ and $670\text{--}690\text{-cm}^{-1}$ regions, respectively.^{27,28} That the $\nu_{\text{as}}(\text{MoOMo})$ bands of $[\text{Mo}_2\text{O}(\text{S}_2\text{CNR}_2)_6]\text{X}$ do not occur in either of these regions is presumably due to the unique electronic and structural features of these compounds.

The cyclic voltammogram of **1** in acetonitrile at a HMDE is shown in Figure 1 and exhibits a quasi-reversible ($\Delta E_p = 77\text{ mV}$) cathodic process at $E_o = -0.77\text{ V}$ (process 1,1'). The ratio $i_{\text{ox}}/i_{\text{red}}$ for this process is close to 1.0 even at slow scan rates, indicative of the formation of a stable reduction product. The number of electrons transferred to each molecule of the complex during this process was determined to be 1.2 by controlled-potential (-1.2 V) electrolysis/coulometry in acetonitrile. The result supports the one-electron reduction of $[\text{Mo}_2\text{O}(\text{S}_2\text{CNEt}_2)_6]^+$, the somewhat high value being explained

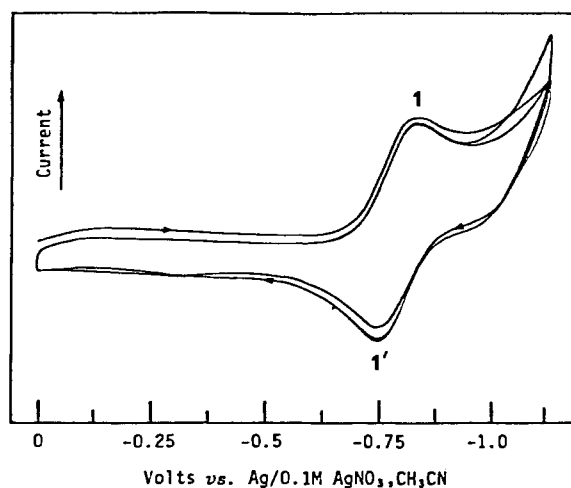
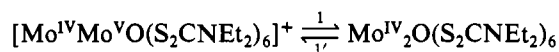


Figure 1. Cyclic voltammogram of $[\text{Mo}_2\text{O}(\text{S}_2\text{CNEt}_2)_6]\text{BF}_4$ in 0.1 M $\text{Et}_4\text{NClO}_4/\text{CH}_3\text{CN}$ at a HMDE (scan rate 100 mV s^{-1}).

by the extreme air sensitivity of the complex in solution. All the above data are consistent with the chemically reversible process



Cyclic voltammetry at a platinum electrode over the potential range from 0.0 to -1.5 V also exhibits a quasi-reversible ($\Delta E_p = 70\text{ mV}$) process analogous to 1,1'. Anodic scanning to $+1.2\text{ V}$ results in three irreversible oxidation peaks at $+0.12$, $+0.45$, and $+0.99\text{ V}$. Subsequent cathodic scans show a new irreversible reduction peak at -0.29 V in addition to process 1,1'. This irreversible reduction peak is associated with an unidentified oxidation product. Thus, electrochemical oxidation of the complex results in irreversible $\mu\text{-oxo}$ -bridge cleavage, also a feature of the aerial oxidation of the complex.

The dinuclear $\mu\text{-oxo}$ -bridged structure suggested by the above data was confirmed by the X-ray crystal structure determination of $[\text{Mo}_2\text{O}(\text{S}_2\text{CNEt}_2)_6]\text{BF}_4$.

The X-ray Crystal Structure of ($\mu\text{-Oxo}$)hexakis(*N,N*-diethyldithiocarbamate)dimolybdenum(IV,V) Tetrafluoroborate (1). In the crystalline state, **1** consists of discrete $[\text{Mo}_2\text{O}(\text{S}_2\text{CNEt}_2)_6]^+$ and BF_4^- ions. In the cation, each molybdenum atom has a distorted pentagonal-bipyramidal (PB) coordination geometry, the PB moieties being linked through the $\mu\text{-oxo}$ ligand. An ORTEP diagram of the complex is given in Figure 2 along with the atom- and ligand-labeling schemes, and a stereodiagram is presented in Figure 3. The tetrafluoroborate

(25) Cromer, D. T.; Liberman, D. *J. Chem. Phys.* **1970**, *53*, 1891.

(26) Geary, W. J. *Coord. Chem. Rev.* **1971**, *7*, 81.

(27) Newton, W. E.; McDonald, J. W. *Reference 10*, p 25.

(28) Mitchell, P. C. H.; Scarle, R. D. *J. Chem. Soc., Dalton Trans.* **1972**, 1809.

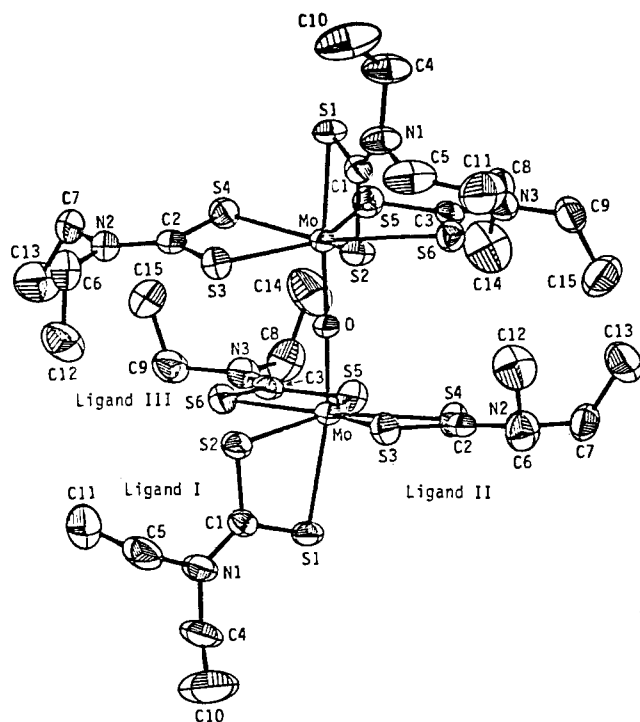


Figure 2. Perspective view of the $[\text{Mo}_2\text{O}(\text{S}_2\text{CNET}_2)_6]^+$ ion. Atoms are shown as ellipsoids of 50% probability, and atom numbers are unbracketed for clarity. Hydrogen atoms have been omitted.

ion is disordered and has been modeled by two distorted tetrahedral forms of equal site occupancy. Both ions have a C_2 symmetry imposed by the space group.

The crystallographically equivalent molybdenum coordination spheres display a distorted pentagonal-bipyramidal geometry with the bridging oxygen atom occupying an axial position; dithiocarbamate ligand I spans the other axial position and one equatorial position, while the remaining equatorial sites accommodate dithiocarbamate ligands II and III. The coordination polyhedron can be described by a set of δ angles²⁹ corresponding to the dihedral angles between the polyhedral faces that intersect along the edges $\text{S}(1)\cdots\text{S}(3)$, $\text{S}(1)\cdots\text{S}(6)$, and the internal "edge" $\text{S}(3)\cdots\text{S}(6)$. With use of equalized metal-ligand bond lengths of 1.0 Å, the calculated δ parameters are 46.3, 49.6, and -80.9° , respectively. A similar set of δ parameters for the corresponding edges on the opposite side of the equatorial plane are 63.5, 61.6, and -63.0° . These normalized δ parameters are in good agreement with those calculated for an idealized D_{5h} PB geometry (54.4, 54.4, and -72.8°).²⁹ The major deviation of the last parameter in both δ sets reflects the primary distortion of the spanning dithiocarbamate ligand. The parameters differ substantially from those calculated for the C_{2v} monocapped trigonal prism (41.4, 0.0, and 0.0°) and the C_{3v} monocapped octahedron (16.2, 16.2, and 16.2°).²⁹ The bond angles subtended at the molybdenum atom also corroborate the PB geometry.³⁰ The principal distortions of the coordination groups from an idealized PB geometry are shown in Figure 4, a view of the MoOS group from an aspect perpendicular to the quasi mirror plane defined by atoms Mo, O, S(1), and S(2) (mean atom displacement 0.019 Å). The equatorial plane is defined by atoms Mo, S(3), S(4), S(5), and S(6),³¹ these atoms having a mean displacement from the plane of 0.026 Å. The dihedral angle between

the equatorial and quasi-mirror planes closely approximates the ideal PB value of 90° (88.8°). Both O and S(1) atoms are displaced from the quasi-fivefold axis through the molybdenum and perpendicular to the equatorial plane (0.187 (1) Å, ca. 5.8° and 0.268 (1) Å, ca. 6.1° , respectively). Sulfur atom S(2) is 0.576 (1) Å (ca. 13.4°) below the equatorial plane.

Interatomic distances within the molybdenum coordination sphere are given in Table III. In the spanning ligand I, two significantly different (6σ) Mo-S bond lengths are observed, these being the shortest (2.484 (3) Å) and longest (2.526 (2) Å) bonds of this type in the molecule. The distances between adjacent sulfur atoms in the equatorial girdle range from 2.815 (2) to 3.054 (2) Å, all of which are much shorter than the sum of the van der Waals radii for sulfur (3.54 Å³²). Interatomic distances between equatorial and axial sulfur atoms are of the order of the van der Waals contact distance.

It is interesting to compare the coordination geometries of $[\text{Mo}_2\text{O}(\text{S}_2\text{CNET}_2)_6]^+$ and the mononuclear complex $[\text{MoO}(\text{S}_2\text{CNET}_2)_3]^+$.³³ First, the equatorial regions of $[\text{Mo}_2\text{O}(\text{S}_2\text{CNET}_2)_6]^+$ are considerably less distorted than that of $[\text{MoO}(\text{S}_2\text{CNET}_2)_3]^+$. In $[\text{Mo}_2\text{O}(\text{S}_2\text{CNET}_2)_6]^+$, the molybdenum atoms are coplanar (displacement 0.0030 (3) Å) with the planes defined by sulfur atoms S(3) to S(6), as reflected in the dihedral angle (2.6°) between the MoS₂ planes of the equatorial ligands II and III. In contrast, the molybdenum atom in $[\text{MoO}(\text{S}_2\text{CNET}_2)_3]^+$ is 0.26 Å above the corresponding tetrasulfur plane due to the movement of the Mo-S bonds away from the Mo-O_i group (dihedral angle between MoS₂ planes 14.5°). In both complexes the average O \cdots S_{eq} interatomic distance is 3.18 (11) Å, indicating that the major cause of the $[\text{MoO}(\text{S}_2\text{CNET}_2)_3]^+$ distortion is the short bond distance (1.684 (6) Å) of the multiply bonded terminal oxo ligand. The single-bonded (see later) μ -oxo ligand is both sterically and electronically incapable of distorting the equatorial plane in $[\text{Mo}_2\text{O}(\text{S}_2\text{CNET}_2)_6]^+$, despite any steric relief this may offer to the molecule. Second, the Mo-S bonds trans to the μ -oxo ligand in $[\text{Mo}_2\text{O}(\text{S}_2\text{CNET}_2)_6]^+$ are considerably shorter than the corresponding bond in $[\text{MoO}(\text{S}_2\text{CNET}_2)_3]^+$ (2.526 (2) and 2.630 (2) Å, respectively). The similar average S_{eq} \cdots S_{ax} interatomic distances in both complexes suggest that the displacement of the equatorial girdle away from the Mo-O_i group in $[\text{MoO}(\text{S}_2\text{CNET}_2)_3]^+$ make a steric contribution to the lengthening of the Mo-S_{ax} bond in this case. The strong electronic trans influence of the multiply bonded Mo-O_i group³⁴ also contributes to the lengthening of the Mo-S_{ax} bond in $[\text{MoO}(\text{S}_2\text{CNET}_2)_3]^+$.

Bond lengths and angles within the dithiocarbamate ligands (Table IV) are consistent with the values found for other related dithiocarbamate complexes.^{33,35} The bite characteristics of the equatorial ligands II and III are similar; however, the unique spanning ligand I exhibits an increased bite and bite angle. A slight inequality of the S-C bond lengths of the ligands, similar to that previously reported,^{33,35} is also observed. The C-N(av) (1.319 (5) Å) and C-S(av) (1.72 (2) Å) bond distances are intermediate between respective single- and double-bond distances (C-N = 1.47 Å, C=N = 1.27 Å, C=S = 1.81 Å, C=S = 1.61 Å³⁶) indicative of delocalized

(29) Muetterties, E. L.; Guggenberger, L. J. *J. Am. Chem. Soc.* **1974**, *96*, 1748; **1977**, *99* 3893.

(30) Drew, M. G. B. *Prog. Inorg. Chem.* **1977**, *23*, 67.

(31) In this paper "equatorial plane" refers to these coplanar atoms, whereas "equatorial girdle" refers to atoms S(2) to S(6). Also, eq = equatorial and ax = axial.

(32) Van der Helm, D.; Lessor, A. E., Jr.; Merritt, L. L., Jr. *Acta Crystallogr.* **1962**, *15*, 1227.

(33) Dirand, J.; Ricard, L.; Weiss, R. *Transition Met. Chem. (Weinheim, Ger.)* **1975**, *1*, 2.

(34) Stiefel, E. I. *Prog. Inorg. Chem.* **1977**, *22*, 1.

(35) Dewan, J. C.; Kepert, D. L.; Raston, C. L.; Taylor, D.; White, A. H.; Maslen, E. N. *J. Chem. Soc., Dalton Trans.* **1973**, 2082. Dirand, J.; Ricard, L.; Weiss, R. *Ibid.* **1976**, 278. Bishop, M. W.; Chatt, J.; Dilworth, J. R.; Neaves, B. D.; Dahlstrom, P.; Hyde, J.; Zubieta, J. J. *Organomet. Chem.* **1981**, *213*, 109 and references therein.

(36) Pauling, L. "The Nature of the Chemical Bond", 3rd ed.; Cornell University Press: Ithaca, NY, 1960; p 260.

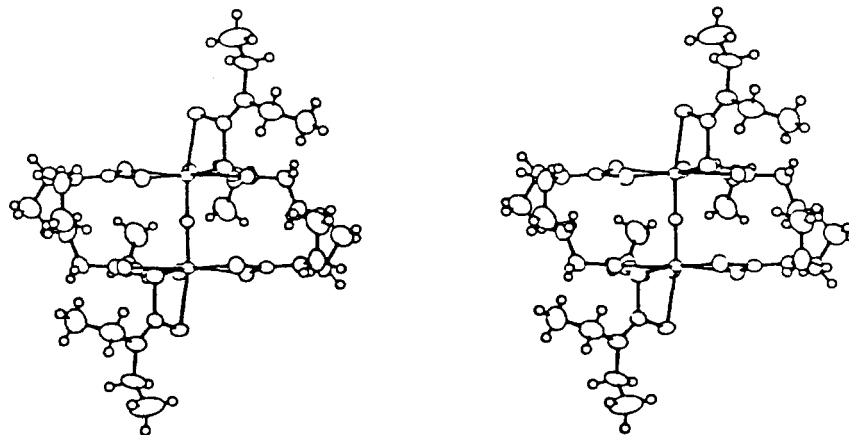


Figure 3. Stereoscopic view of $[\text{Mo}_2\text{O}(\text{S}_2\text{CNET}_2)_6]^+$ along the C_2 axis. Non-hydrogen atoms are shown as ellipsoids of 50% probability. Hydrogen atoms are spheres of convenient arbitrary size.

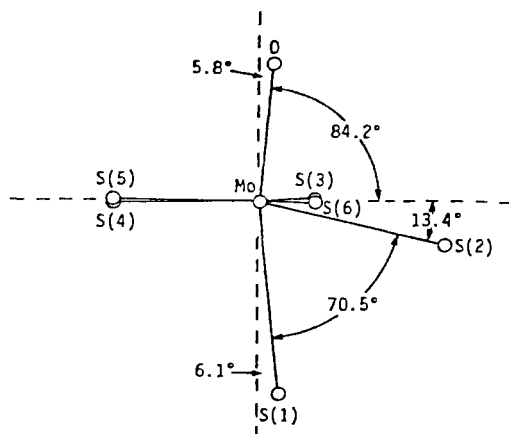


Figure 4. Principal distortions of the MoOS_6 coordination group of $[\text{Mo}_2\text{O}(\text{S}_2\text{CNET}_2)_6]^+$. The quasi mirror plane lies in the plane of the paper.

π bonding in the S_2CN portion of the ligands. The six atoms defining the rigid S_2CNC_2 skeleton of the ligands are nearly coplanar for each ligand, the maximum displacement of these atoms from their respective mean planes being 0.068 (5) Å. The ethyl substituents of ligands II and III are syn, whereas those of ligand I are anti. The syn conformation is dictated by crystal packing forces and is rarely observed in dithiocarbamate complexes, being present in only two previously reported seven-coordinate tris(dithiocarbamate) complexes, $\text{TaS}(\text{S}_2\text{CNET}_2)_3$ ³⁷ and $\text{Te}(\text{S}_2\text{CNET}_2)_3\text{Ph}$.³⁸

The $[\text{Mo}_2\text{O}(\text{S}_2\text{CNET}_2)_6]^+$ complex is composed of two PB asymmetric units linked via the near-linear ($\text{MoOMo} = 175.6$ (2)°) bridging oxo ligand. The bond length (1.848 (2) Å) and angle of the μ -oxo ligand are typical of similar features in previously reported structures, the bond length and angle ranges for μ -oxo molybdenum complexes being 1.851–1.936 Å and 136.1–180°, respectively.^{11,40} The Mo–O bond length is consistent with a Mo–O order of 1 in $[\text{Mo}_2\text{O}(\text{S}_2\text{CNET}_2)_6]^+$.⁴¹

The equatorial planes of the PB moieties are nearly perpendicular to the Mo_2O plane, the dihedral angles being 93.6°.

However, the equatorial planes are tilted by 13.6° with respect to each other. This is reflected in the closer approach of the intergirdle S(2), S(3) pairs (3.842 (2) Å) compared to the S(4), S(6) and S(5) pairs (3.957 (2) and 4.210 (2) Å, respectively). The sulfur atoms of the two equatorial girdles occupy nearly eclipsed positions. When viewed along the Mo...Mo vector, sulfur atoms S(4) and S(6) are only ca. 2° from a fully eclipsed position, while pairs S(2), S(3) and S(5), S(5) are less eclipsed (by ca. 9 and 8°, respectively). The equatorial ligands are "staggered" with respect to one another allowing the syn ethyl substituents to occupy alternating positions between the equatorial planes. This conformation, dictated by intramolecular forces, results in very short non-bonded methyl contacts: C(12)...C(13), 3.39 (1) Å; C(14)...C(15), 3.35 (1) Å; C(11)...C(12)*, 3.86 (1) Å; C(13)...C(15)*, 3.65 (1) Å; C(14)...C(14)*, 3.85 (1) Å (asterisk denotes atom of adjoining asymmetry unit).

The structure of $[\text{Mo}_2\text{O}(\text{S}_2\text{CNET}_2)_6]^+$ is unique in μ -oxo (dithiocarbamate)molybdenum chemistry, being the first dimeric seven-coordinate complex of this type and the first dithiocarbamate complex to exhibit μ -oxo bridging in the absence of terminal oxo ligation. As well, the complex is the first example of a μ -oxo molybdenum complex in which the metal atoms are bridged by a single axial oxygen atom. Other axially bridged PB complexes of molybdenum are known; these include the fluoro-bridged $[\text{MoO}(\text{O}_2)(\text{dipic})_2\text{F}]$ ⁴² and the sulfido-bridged $[\text{Mo}(\text{CN})_6]_2\text{S}$ ^{6+,43}.

The packing of the ions within the unit cell is shown in Figure 5. The influence of the crystal packing on the dithiocarbamate ligand substituent conformations is readily appreciated. Only one intermolecular contact is significantly shorter than the van der Waals contact distance of 3.4 Å,³⁶ i.e., C(11)...F(1) = 3.20 (1) Å.

Electronic Spectral Data and the Nature of the Mixed Oxidation State. The degree of oxidation-state delocalization is an important feature of mixed-oxidation-state compounds and has been used by Robin and Day⁴⁴ as a criterion for classification. The Robin and Day scheme, modified since its inception,⁴⁵ recognizes three classes of dinuclear compounds.

Class I. The oxidation states are strongly localized on crystallographically distinct metal sites, and the properties of the compounds are essentially a superposition of those of the constituent metal centers. The intervalence-transfer (IT = $[a,b] \rightarrow [b,a]^*$ ⁴⁶) bands are of high energy ($>27\,000\text{ cm}^{-1}$),

(37) Peterson, E. J.; von Dreeble, R. B.; Brown, T. M. *Inorg. Chem.* **1978**, *17*, 1410.

(38) Esperas, S.; Husebye, S. *Acta Chem. Scand.* **1972**, *26*, 3293.

(39) Day, V. W.; Fredrick, M. F.; Klemperer, W. G.; Shum, W. *J. Am. Chem. Soc.* **1977**, *99*, 6146. DeSimone, R. E.; Cragel, J., Jr.; Ilesley, W. H.; Glick, M. D.; *J. Coord. Chem.* **1979**, *9*, 167. LeCarpentier, J.-M.; Mitschler, A.; Weiss, R. *Acta Crystallogr., Sect. B* **1972**, *B28*, 1288. Stromberg, R. *Acta Chem. Scand.* **1968**, *22*, 1076. Glowiak, T.; Rudolf, M. F.; Sabat, M.; Jezowska-Trzebiatowska, B. Reference 10, p 17.

(40) Ricard, L.; Estienne, J.; Karagiannidis, P.; Toledano, P.; Fischer, J.; Mitschler, A.; Weiss, R. *J. Coord. Chem.* **1974**, *3*, 277. Zubieta, J.; Maniloff, G. B. *Inorg. Nucl. Chem. Lett.* **1976**, *12*, 121.

(41) Schroder, F. A. *Acta Crystallogr., Sect. B* **1975**, *B31*, 2294.

(42) Edwards, A. J.; Slim, D. R.; Guerchais, J. E.; Kergoat, R. *J. Chem. Soc., Dalton Trans.* **1980**, 289.

(43) Drew, M. G. B.; Mitchell, P. C. H.; Pygall, C. F. *J. Chem. Soc., Dalton Trans.* **1979**, 1213.

(44) Robin, M. B.; Day, P. *Adv. Inorg. Chem. Radiochem.* **1967**, *10*, 247.

(45) Wong, K. Y.; Schatz, P. N. *Prog. Inorg. Chem.* **1981**, *28*, 369.

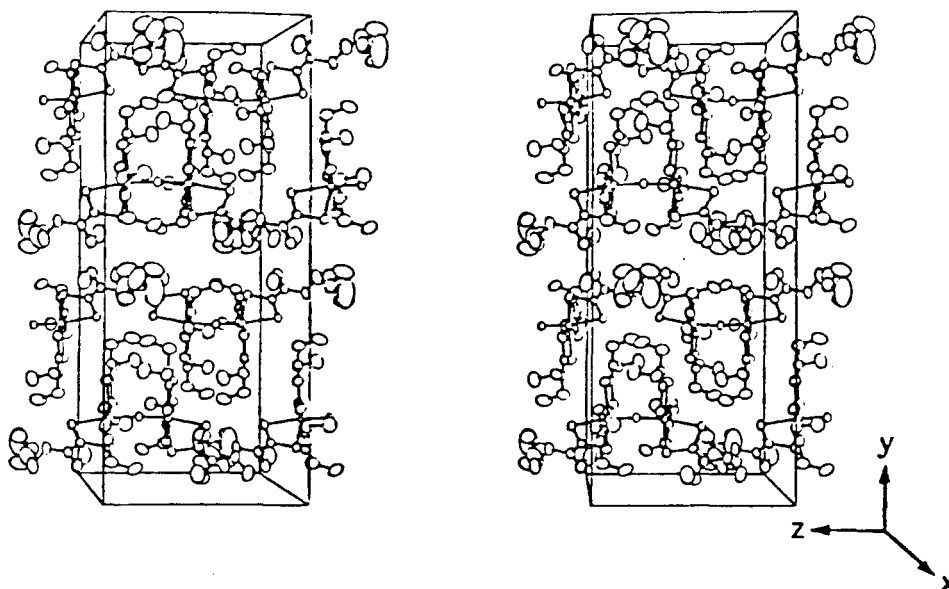


Figure 5. Stereoscopic packing diagram of $[\text{Mo}_2\text{O}(\text{S}_2\text{CNET}_2)_6]\text{BF}_4$. Ellipsoids represent 50% probability. The hydrogen atoms have been omitted.

reflecting the gross structural or electronic differences between the metal centers.

Class II. The metal ions are in crystallographically similar or identical coordination environments and possess distinguishable although slightly delocalized oxidation states. The compounds exhibit IT bands in the visible region and spectroscopic properties that exhibit some characteristics of the constituent metal ions.

Class IIIA. The metal ions are crystallographically indistinguishable, and oxidation-state delocalization is complete. The compounds exhibit low-energy absorption bands associated with the mixed-oxidation-state formulation and other properties that are distinctly different from those of the constituent ions.

The properties of **1** support its classification as a class IIIA compound in which the molybdenum atoms possess an average oxidation state of 4.5+. In the crystal structure of the compound, the equivalence of the molybdenum sites is consistent with, but not conclusive evidence for, a class IIIA classification. Quite clearly a class I complex may be discounted. However, the thermal motion of the atoms within the coordination sphere is sufficiently large (rms amplitude range 0.15–0.24 Å) to conceal the presence of a class II type molybdenum-site inequivalence. For this to be the case, the localized Mo(V) and Mo(IV) sites, which are undergoing rapid intervalence transfer, must both exhibit PB coordination spheres with bond lengths differing by less than the rms amplitude observed. However, several features of the structure favor the strict metal equivalence of a class IIIA formulation. First, the PB coordination geometry of $[\text{Mo}_2\text{O}(\text{S}_2\text{CNET}_2)_6]^+$ and the lack of structurally characterized PB Mo(V) complexes suggest that the coordination spheres of localized Mo(IV) and Mo(V) ions would show a greater structural disparity than is consistent with the thermal parameters of $[\text{Mo}_2\text{O}(\text{S}_2\text{CNET}_2)_6]^+$. Second, these parameters are very similar to those reported for mononuclear (dithiocarbamato)molybdenum complexes in which unusual dynamic motion is absent;^{33,35} i.e., the thermal motion of the complex may be readily accounted for by the “natural” vibration of the constituent atoms alone. In particular, the thermal parameters of the molybdenum and oxygen atoms show *no unusual features*. Further, the symmetrical packing

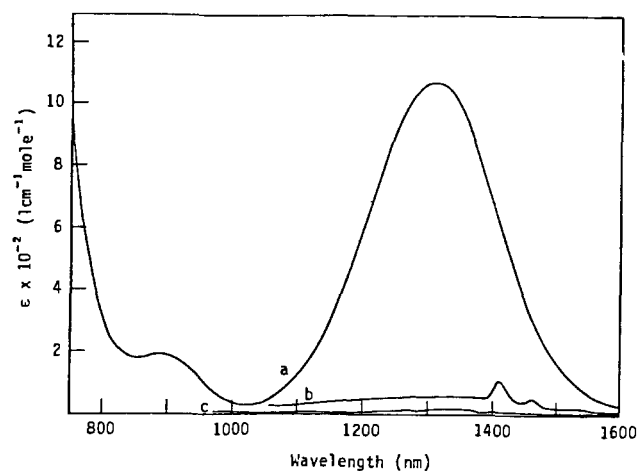
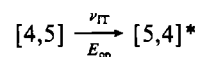


Figure 6. Near-infrared spectra of (a) $[\text{Mo}_2\text{O}(\text{S}_2\text{CNET}_2)_6]\text{BF}_4$ in acetonitrile, (b) $\text{Mo}_2\text{O}(\text{S}_2\text{CNET}_2)_6$ in 0.1 M Et_4NClO_4 /acetonitrile, and (c) solution following aerial oxidation.

of the BF_4^- counterions with respect to the molybdenum centers in $[\text{Mo}_2\text{O}(\text{S}_2\text{CNET}_2)_6]^+$ suggests equivalent metal charge densities and again favors a class IIIA formulation.

A low-energy absorption band is a conspicuous feature of the electronic spectra of both class II and class IIIA compounds; **1** is no exception and exhibits a well-defined absorption at 1310 nm (7630 cm^{-1}). This band (Figure 6) may be assigned to an electronic transition uniquely associated with the mixed-oxidation-state complex, as it is absent from both the spectra of the one-electron reduction product, presumably $\text{Mo}_2\text{O}(\text{S}_2\text{CNET}_2)_6$, and air-oxidized solutions of **1**.

Since the origin of the 1310-nm band is determined by the ground and excited electronic states of the complex, its properties should provide valuable information on the degree of oxidation-state delocalization. In a class II system, the band would represent the intervalence-transfer (IT) transition



Here, the optical transition occurs instantaneously on the vibrational time scale, resulting in Mo(IV) and Mo(V) ions in the equilibrium coordination spheres of the other oxidation state. Thus, the energy between the ground and excited mixed-oxidation states, E_{op} , is determined by the excess vi-

(46) In the $[a,b]$ state, the metal ions in coordination sites A and B have oxidation states of a and b , respectively. In the $[b,a]$ state these sites contain metal ions of oxidation states b and a , respectively.

Table V. Near-Infrared Spectral Data for $[\text{Mo}_2\text{O}(\text{S}_2\text{CNET}_2)_6]\text{BF}_4$

solvent	$1/D_{\text{op}} - 1/D_s^a$	λ_{max} , nm (ν_{max} , cm^{-1})	ϵ , L cm^{-1} mol^{-1}	$\Delta\nu_{1/2}^b$, cm^{-1}
CH_3CN^c	0.526	1310 (7630)	1100	1380
		890 (11 230)	220	
$\text{C}_4\text{H}_6\text{O}_3^d$	0.481	1310 (7630)	1090	1400
		890 (11 230)	220	
$(\text{CH}_3)_2\text{SO}$	0.438	1310 (7630)	1140	1390
		890 (11 230)	230	
$\text{C}_6\text{H}_5\text{NO}_2$	0.384	1310 (7630)	1160	1400
		890 (11 230)	230	
CHCl_3^d		1310 (7630)	1100	1380
		890	220	

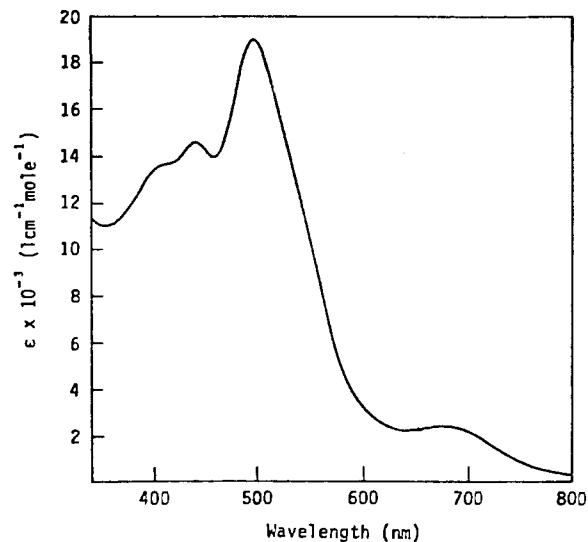
^a Gordon, A. J.; Ford, R. A. "The Chemists Companion"; Wiley-Interscience: New York, 1972; pp 4-11. ^b Bandwidth at half-height; the 890-nm band is a shoulder. ^c In this solution, Beer's Law is obeyed over the concentration 2.5×10^{-4} to 3.4×10^{-3} M. ^d Propylene carbonate.

brational energy content of the excited state over that of the ground state. A theoretical treatment of class II IT bands has been developed by Hush⁴⁷ and has been verified by many studies of localized class II (Ru(II, III) complexes.⁴⁸ For a class IIIA system, the band would represent an electronic transition between the ground- and excited-state molecular orbitals of a completely delocalized $[4^{1/2}, 4^{1/2}]$ complex. Hush's theory is inappropriate for the description of bands of this origin.

The properties of the 1310-nm band deviate considerably from those predicted by Hush for class II systems, clearly supporting the alternative class IIIA formulation. According to Hush, the lower limit for the bandwidth of a class II IT band (at 300 K) is given by $\nu_{\text{max}} = (\Delta\nu_{1/2})^2/2310$ where ν_{max} is the energy of the IT band and $\Delta\nu_{1/2}$ is the bandwidth at half-height. Since ν_{max} is 7630 cm^{-1} , the calculated value for $\Delta\nu_{1/2}$ is 4200 cm^{-1} , which is much larger than the observed value of 1390 cm^{-1} . Also, the energy of the IT band in class II complexes is predicted to be solvent dependent as both inner-sphere (λ_i) and outer-sphere (solvent) vibrational modes (λ_o) contribute to the excess vibrational energy of the IT excited state. For a symmetric dinuclear complex, E_{op} is given by

$$E_{\text{op}} = \lambda_i + \lambda_o = \lambda_i + (me)^2 \left(\frac{a_1}{2} + \frac{a_2}{2} - \frac{1}{d} \right) \left(\frac{1}{D_{\text{op}}} - \frac{1}{D_s} \right)$$

where m is the extent of charge transfer in the IT process, e is the unit electron charge, a_1 and a_2 are the nuclear radii of the electron donor and acceptor sites, d is the internuclear site separation, and D_{op} and D_s are the optical and static dielectric constants of the medium. This equation predicts a linear variation of E_{op} with changing solvent dielectric properties ($1/D_{\text{op}} - 1/D_s$). However, this solvent dependence may break down if the IT band is sufficiently weak.⁴⁹ In such a case, the relaxation time associated with solvent reorganization is slower than the rate of electron transfer (ca. 10^{10} s^{-1} at room temperature) and the solvent molecules occupy an equilibrium solvent sphere around the complex. At these levels, a localized vs. delocalized description becomes a matter of definition, the usual criterion for delocalization being that the lifetime of a particular mixed oxidation state is shorter than the vibrational time scale (ca. 10^{-13} s). In the near-infrared spectra of **1** (Table V), the insensitivity of ν_{max} to the dielectric properties of the medium strongly suggests that the charge distribution

Figure 7. Electronic spectrum of $[\text{Mo}_2\text{O}(\text{S}_2\text{CNET}_2)_6]\text{BF}_4$ in methanol.

is symmetrical and essentially the same in the ground and excited states, as expected for a class IIIA system. Certainly, the rate of electron transfer between sites exceeds ca. 10^{10} s^{-1} .

The electronic spectrum of the compound in the visible region (Figure 7) also supports a class IIIA formulation, as the intense absorption bands at 677 (2440), 497 (19 200), 440 (14 400), and 410 nm ($13 400 \text{ L cm}^{-1} \text{ mol}^{-1}$) cannot be attributed to discrete Mo(IV) and Mo(V) centers. The absorption bands follow Beer's law over the accessible concentration range (1.5×10^{-4} to 2.1×10^{-5} M), supporting the integrity of the dinuclear species in solution. Following the one-electron reduction of **1** in 0.1 M $\text{Et}_4\text{NClO}_4/\text{CH}_3\text{CN}$, the spectrum shifts to slightly shorter wavelengths and is much less intense (λ_{max} , nm (ϵ , $\text{L cm}^{-1} \text{ mol}^{-1}$): 668 (570), 494 (7180), 441 (6510), 400 (6400), respectively). The similarity of the spectra of $[\text{Mo}_2\text{O}(\text{S}_2\text{CNET}_2)_6]^+$ and $\text{Mo}_2\text{O}(\text{S}_2\text{CNET}_2)_6$ suggests that each complex could be described by a similar molecular orbital scheme. Also the short metal-metal distance and the participation of the oxygen p orbitals in Mo-O-Mo π bonding would facilitate strong metal interactions similar to those observed in other second- and third-row transition-metal μ -oxo complexes, e.g. in the μ -oxo ruthenium(III) complexes $[\text{L}_2\text{XRuORuXL}_2]^{n+}$ (where L = bpy, phen; X = Cl^- , NO_2^- , H_2O) and the mixed-oxidation-state complex $[(\text{bpy})_2\text{ClRuORuCl}(\text{bpy})_2]^{3+}$.⁵⁰ Notably, the crystallographic and electronic spectral properties of $[\text{Mo}_2\text{O}(\text{S}_2\text{CNET}_2)_6]^+$ are strikingly similar to those of the well-known Creutz-Taube (C-T) complex $[(\text{NH}_3)_3\text{Ru}(\text{pyz})\text{Ru}(\text{NH}_3)_3]^{5+}$,⁵¹ with both complexes possessing crystallographically equivalent metal centers and exhibiting near-infrared spectra atypical of class II systems.

The only previous example of a mixed-oxidation-state complex of this type is $[\text{Mo}_2\text{O}_3(\text{S}_2\text{CNET}_2)_4]^-$. Electrochemical studies indicate that this anion has only a transient existence in solution.⁹ In contrast, **1** is a pure, stable, and preparatively reproducible mixed-oxidation-state oxo and sulfur donor ligand compound of molybdenum. The stability of the complex may be explained in part by the high sulfur content of the coordination sphere as the stability of transient electrochemically produced Mo(IV, V) complexes has been observed to increase with increasing sulfur coordination.^{9a,b} The high sulfur content of molybdoenzyme active sites may thus favor the formation of mixed-oxidation-state centers during catalysis; the work

(47) Hush, N. S. *Prog. Inorg. Chem.* **1967**, *8*, 391.(48) Meyer, T. J. *Acc. Chem. Res.* **1978**, *11*, 94.(49) Bunker, B. C.; Drago, R. S.; Hendrickson, D. N.; Richman, R. M.; Kessell, S. L. *J. Am. Chem. Soc.* **1978**, *100*, 3805.(50) Weaver, T. R.; Meyer, T. J.; Adeyemi, S. A.; Brown, G. M.; Eckberg, R. P.; Hatfield, W. E.; Johnson, E. C.; Murray, R. W.; Untereker, D. *J. Am. Chem. Soc.* **1975**, *97*, 3039.(51) Creutz, C.; Taube, H. *J. Am. Chem. Soc.* **1973**, *95*, 1086.

described here shows that such centers are certainly capable of existence should the molybdenum atoms in molybdoenzymes be closely associated. It may also be noted that $[\text{Mo}_2\text{O}(\text{S}_2\text{CNEt}_2)_6]^+$ is formed from, and is oxidized to, two mononuclear metal centers, thus showing similarity to Wentworth's proposed formation and oxidation of dinuclear enzyme centers.²

Acknowledgment. We are indebted to Dr. G. B. Robertson and G. M. McLaughlin for access to the diffractometer and ANUCRYS program library and for helpful discussions.

Registry No. 1, 88253-60-5; 2, 88293-52-1; 3, 88293-53-2; 4, 88293-54-3; $[\text{Mo}_2\text{O}(\text{S}_2\text{CNMe}_2)_6]\text{BF}_4$, 88253-62-7; $[\text{Mo}_2\text{O}(\text{S}_2\text{CNMe}_2)_6]\text{ClO}_4$, 88293-55-4; $[\text{MoO}(\text{S}_2\text{CNEt}_2)_3]\text{BF}_4$, 70788-19-1; $\text{MoCl}(\text{S}_2\text{CNEt}_2)_3$, 84493-50-5; triphenylphosphine, 603-35-0.

Supplementary Material Available: Tables containing thermal parameters of non-hydrogen atoms, calculated hydrogen atom parameters, additional bond lengths, bond angles, and interatomic distances, least-squares planes and related dihedral angles, geometrical parameters for the tetrafluoroborate ion, and parameters for reduction of compound 1 (7 pages). Ordering information is given on any current masthead page.

Contribution from the Chemical Crystallography Laboratory, Oxford University, Oxford OXI 3PD, England, Department of Inorganic Chemistry, Bristol University, Bristol BS8 ITS, England, and Department of Chemistry, Rider College, Lawrenceville, New Jersey 08648

Preparation and Crystal Structure of $\text{La}_3\text{Mo}_4\text{SiO}_{14}$, an Unusual Cluster Compound of Molybdenum

P. W. BETTERIDGE,^{1a} A. K. CHEETHAM,^{1a} J. A. K. HOWARD,^{1b} G. JAKUBICKI,^{1c} and W. H. MCCARROLL*^{1c}

Received August 19, 1982

Black needles of $\text{La}_3\text{Mo}_4\text{SiO}_{14}$ (average Mo oxidation state: 3.75) were prepared by electrolytic reduction at 1100 °C of a melt containing Na_2MoO_4 , MoO_3 , and La_2O_3 . The silicon was abstracted from the porcelain crucible. The compound crystallizes in orthorhombic space group *Pnma* with $a = 17.684$ (4) Å, $b = 5.643$ (1) Å, $c = 11.037$ (2) Å, $V = 1101.4$ (5) Å³, and $Z = 4$. Diffraction data (Mo $K\alpha$ radiation, $2\theta(\text{max}) = 60^\circ$) were collected on a Syntex P2₁ automated diffractometer, and the structure was refined by blocked-cascade full-matrix least-squares methods to $R_F = 4.2\%$ and $R_{wF} = 4.5\%$ with use of 1755 independent reflections. The structure contains triangular Mo_3O_{13} units with Mo-Mo distances of 2.550 (1) and 2.562 (1) Å and edge-sharing MoO_6 octahedra with Mo-Mo distances alternately 2.551 (1) and 3.13 (1) Å along the chain direction. The Si is tetrahedrally coordinated (mean Si-O distance: 1.64 Å), and the three crystallographically distinct La atoms have coordination numbers of 8, 9, and 10, the stereochemistry in each case being based upon trigonal-prismatic coordination.

Introduction

Examples of mixed-metal oxides in which molybdenum adopts a formal oxidation state of 4 or less are comparatively few. Among the more interesting mixed Mo(IV) oxides are $\text{M}_2\text{Mo}_3\text{O}_8$ ($M = \text{Mg}, \text{Mn}, \text{Fe}, \text{Co}, \text{Ni}, \text{Zn}, \text{Cd}$),² which contain the Mo_3O_{13} unit. This unit has a triangle of molybdenum atoms joined by Mo-Mo bonds. Other Mo(IV) oxides are known, but structural information is more limited. Among compounds in which Mo is yet further reduced, Reau et al.³ have reported the preparation of $\text{Na}_2\text{Mo}_3\text{O}_6$ with an average Mo oxidation state 3.33, but this compound has been prepared only as a polycrystalline material and its crystal structure is not known. Recently, Torardi and McCarley have reported the preparation and structure of, for example, $\text{LiZn}_2\text{Mo}_3\text{O}_8$,⁴ NaMo_4O_6 ,⁵ and $\text{Ba}_{0.62}\text{Mo}_4\text{O}_6$ ⁶ with average oxidation states for Mo of 3.67, 2.75, and 2.69, respectively. The lithium compound contains a Mo_3O_{13} cluster while the sodium and barium compounds contain octahedral units, Mo_6O_8 .

In the belief that these cluster compounds are not isolated examples but are representative of a large family of oxides containing molybdenum in low formal oxidation states, we are undertaking a program aimed at preparing such materials by both solid-state and electrolytic reactions. The latter method has been particularly useful for the preparation of tungsten

and molybdenum oxide bronzes⁷ and appeared particularly appropriate for our endeavors. Here we report the preparation and crystal structure of $\text{La}_3\text{Mo}_4\text{SiO}_{14}$, a compound with an average Mo oxidation state of 3.75, which contains two distinct structural elements of molybdenum.

Experimental Section

Synthesis and Analysis. All chemicals used in these syntheses were of reagent grade or better. MoO_3 was ignited at 475 °C before use, while La_2O_3 and Nd_2O_3 were treated similarly at 1000 °C. Single crystals of the title compound were prepared by the electrolysis of a melt formed at 1100 ± 10 °C from a mixture of sodium molybdate, molybdenum(VI) oxide, and lanthanum oxide. The reactants were weighed to the nearest 0.01 g and mixed carefully before heating. Typical charges weighed from 25 to 35 g. Smooth platinum-foil electrodes with a nominal surface area of 2 cm² were used, and the charge was contained in a Coors porcelain crucible. Although the title compound forms over the range of molar ratios of $\text{Na}_2\text{MoO}_4:\text{MoO}_3:\text{La}_2\text{O}_3 = (3.50-3.00):(3.50-3.00):1.00$, reactions at the extremes produce multiphase products and the optimum ratios appear to be about 3.10:3.10:1.00. After the operating temperature was reached, the melt was allowed to equilibrate for 1 h before electrolysis began. Typically, a constant current of 200 mA was passed for 30-40 min. The electrolysis was carried out without a protective atmosphere and was terminated by removing the electrodes from the melt and allowing them to cool to room temperature. The black needles, which grow from the cathode in clusters, were separated from the solidified matrix by washing alternately with hot 5% potassium carbonate solution and hot 2 M hydrochloric acid. Washings were continued until all of the molybdate matrix was removed and the acid washings no longer turned blue, indicating that all the soluble reduced products had been removed. The yield of purified product was small,

- (1) (a) Oxford University. (b) Bristol University. (c) Rider College.
- (2) (a) McCarroll, W. H.; Katz, L.; Ward, R. *J. Am. Chem. Soc.* **1957**, *79*, 5410. (b) Ansell, G. B.; Katz, L. *Acta Crystallogr.* **1966**, *21*, 482.
- (3) Reau, J. M.; Fouassier, C.; Hagenmuller, P. *Bull. Soc. Chim. Fr.* **1970**, 3827.
- (4) Torardi, C. C. Ph.D. Dissertation, Iowa State University, Ames, IA, 1981.
- (5) Torardi, C. C.; McCarley, R. E. *J. Am. Chem. Soc.* **1979**, *101*, 3963.
- (6) Torardi, C. C.; McCarley, R. E. *J. Solid State Chem.* **1981**, *37*, 393.

- (7) Banks, E.; Wold, A. "Preparative Inorganic Reactions"; Wiley: New York, 1968; Vol. 4, p 237.